Biogeosciences, 20, 1–14, 2023
https://doi.org/10.5194/bg-20-1-2023

Biogeosciences Open Access EGU

Ice nucleating properties of the sea ice diatom *Fragilariopsis cylindrus* and its exudates

Lukas Eickhoff[1], Maddalena Bayer-Giraldi[2,a], Naama Reicher[3], Yinon Rudich[3], and Thomas Koop[1]

[1]Faculty of Chemistry, Bielefeld University, 33615 Bielefeld, Germany
[2]Faculty of Mathematics, Informatics and Natural Sciences, Universität Hamburg, 20354 Hamburg, Germany
[3]Department of Earth and Planetary Sciences, Weizmann Institute of Science, 76100 Rehovot, Israel
[a]formerly at: Alfred Wegener Institute, Helmholtz Centre for Polar and Marine Research, 27568 Bremerhaven, Germany

Correspondence: Thomas Koop (thomas.koop@uni-bielefeld.de)

Received: 3 May 2022 – Discussion started: 18 May 2022
Revised: 7 October 2022 – Accepted: 15 November 2022 – Published: 2 January 2023

Abstract. In this study, we investigated the ice nucleation activity of the Antarctic sea ice diatom *Fragilariopsis cylindrus*. Diatoms are the main primary producers of organic carbon in the Southern Ocean, and the Antarctic sea ice diatom *F. cylindrus* is one of the predominant species. This psychrophilic diatom is abundant in open waters and within sea ice. It has developed several mechanisms to cope with the extreme conditions of its environment, for example, the production of ice-binding proteins (IBPs) and extracellular polymeric substances known to alter the structure of ice. Here, we investigated the ice nucleation activity of *F. cylindrus* using a microfluidic device containing individual sub-nanolitre ($\sim 90\,\mu m$) droplet samples. The experimental method and a newly implemented Poisson-statistics-based data evaluation procedure applicable to samples with low ice nucleating particle concentrations were validated by comparative ice nucleation experiments with well-investigated bacterial samples from *Pseudomonas syringae* (Snomax®). The experiments reveal an increase of up to 7.2 °C in the ice nucleation temperatures for seawater containing *F. cylindrus* diatoms when compared to pure seawater. Moreover, *F. cylindrus* fragments also show ice nucleation activity, while experiments with the *F. cylindrus* ice-binding protein (*fc*IBP) show no significant ice nucleation activity. A comparison with experimental results from other diatoms suggests a universal behaviour of polar sea ice diatoms, and we provide a diatom-mass-based parameterization of their ice nucleation activity for use in models.

1 Introduction

Sea ice is a two-phase medium composed predominantly of crystalline ice with embedded liquid channels and pockets (inclusions) in which active life can take place. As seawater freezes, dissolved sea salt ions are segregated from the growing ice lattice and accumulate in liquid brine inclusions, which have a lower freezing point due to their high salinity. Its porous structure makes sea ice a habitat for various organisms and enables life within the liquid brine network. Higher irradiance levels in sea ice, when compared to the seawater column, represent an advantage for photosynthetically active microorganisms populating the pore space (Eicken, 1992). During sea ice formation, most microorganisms from the water column remain entrapped within the ice or are scavenged by floating ice crystals (Ackley and Sullivan, 1994). Species composition changes with the ageing of ice and the stabilization of the brine channel system (Krembs and Engel, 2001), resulting in a dominance of diatom species producing sticky extracellular polymeric substances (EPSs) with ice-adhering functions (Raymond et al., 1994).

The diatom *Fragilariopsis cylindrus* (see Fig. 1) is widespread in polar environments and is one of the predominant species within the Arctic and Antarctic microbial assemblages (Kang and Fryxell, 1992; Poulin et al., 2011; van Leeuwe et al., 2018). The species thrives within sea ice, where it can be found along the sea ice column (Bartsch, 1989; Garrison and Buck, 1989; Günther and Dieckmann, 2001; Poulin et al., 2011). It is, therefore, considered to be an indicator of sea ice extent in palaeoenvironmental studies for

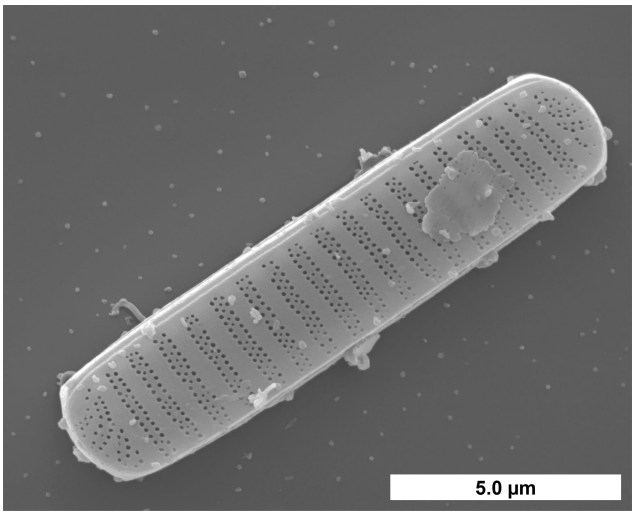

Figure 1. *F. cylindrus* cell visualized by scanning electron microscopy. (Image courtesy of Henrik Lange and Friedel Hinz, Alfred Wegener Institute, Germany).

reconstructions of past variations (Gersonde and Zielinski, 2000). *F. cylindrus* is also abundant in the water column, for example, in the proximity of the sea ice edge zone (Kang and Fryxell, 1992; Lizotte, 2001) and in ice-covered waters (Garrison and Buck, 1989). *F. cylindrus* has developed a range of mechanisms for coping with the extreme conditions occurring within sea ice (Mock et al., 2017). One prominent example is the production of so-called ice-binding proteins (IBPs; Bayer-Giraldi et al., 2011) and of other EPSs that are also found in other diatom species (Wilson et al., 2015; Aslam et al., 2018). *F. cylindrus* produces several ice-binding protein (IBP) isoforms (*fc*IBPs), all of which belong to the broadly extended IBP family with a domain of unknown function DUF3494 (Vance et al., 2019). It was shown that *fc*IBP isoform 11 affects the microstructure, i.e. the shape and size, of ice crystals (Bayer-Giraldi et al., 2011, 2018). Moreover, EPSs offer a protective environment to *F. cylindrus* in order to cope with the conditions of the sea ice habitat (Aslam et al., 2012a, b, 2018). It has been suggested that *fc*IBPs accumulate in EPSs and, when in contact with the icy walls of brine inclusions, alter the pore space, resulting in an increased habitability (Bayer-Giraldi et al., 2011).

The very good ice-binding properties of *fc*IBP and EPSs (mainly polysaccharides and proteins) under sea ice brine conditions have been reported in previous studies (Krembs et al., 2002, 2011; Bayer-Giraldi et al., 2011). Ice-binding proteins (IBPs) bind to ice crystal surfaces and, by doing so, can control the crystal growth rate, inhibit ice recrystallization, or help to adhere their host to ice (Davies, 2014; Bar Dolev et al., 2016; Guo et al., 2017). Originally, IBPs were known as antifreeze (glyco)proteins, which protect fish and insects by thermal hysteresis, i.e. by depressing the temperature where active crystal growth occurs to below the equilibrium melting point temperature (Bar Dolev et al., 2016). However, not all IBPs have such thermal hysteresis antifreeze properties. For example, a recently discovered IBP from the Antarctic bacterium *Marinomonas primoryensis* binds its bacterial host to diatoms and the Antarctic sea ice layer (Guo et al., 2017). Furthermore, even ice nucleating proteins are sometimes considered to be a subgroup of IBPs because their active sites appear to be structurally similar, just much larger, than those of regular IBPs with antifreeze properties (Davies, 2014; Bar Dolev et al., 2016; Eickhoff et al., 2019; Hudait et al., 2019). These considerations may imply that the much smaller ice-binding sites of antifreeze IBPs could also stabilize the formation of small ice embryos and thereby promote the nucleation of ice from liquid water; however, this occurs only at very low temperatures (Davies, 2014; Bar Dolev et al., 2016; Eickhoff et al., 2019; Hudait et al., 2019). Indeed, it has been shown both experimentally and in molecular dynamics simulations that the ice-binding antifreeze proteins of the mealworm beetle *Tenebrio molitor* (*tm*AFP) can also trigger the nucleation of new ice crystals just a few degrees Celsius above the homogenous freezing temperature of water or an aqueous solution (Eickhoff et al., 2019; Hudait et al., 2019). Here, we explore whether a similar ice nucleating effect also occurs for IBPs from *F. cylindrus*.

Many biological particles such as bacteria, viruses, or diatoms have been detected in the sea surface microlayer and in the thawing permafrost (Leck and Bigg, 2005; Wilson et al., 2015; Irish et al., 2017; Creamean et al., 2020; Ickes et al., 2020; Roy et al., 2021). Some of these biological particles can increase the ice nucleation temperature of small water droplets and act as ice nucleating particles (INPs; DeMott et al., 2016; Ickes et al., 2020; Welti et al., 2020; Creamean et al., 2021; Hartmann et al., 2021; Roy et al., 2021). These biological particles can be transported to the atmospheric boundary layer by sea spray aerosol droplets (Irish et al., 2019; Steinke et al., 2022). In the polar atmosphere, they can be transported over long distances (Šantl-Temkiv et al., 2019, 2020). Sea spray aerosol contributes to ice nucleation under mixed-phase cloud conditions and at cirrus temperatures in the upper troposphere (DeMott et al., 2016; Hartmann et al., 2021; Wagner et al., 2021). Further experiments on diatoms and their EPSs show that they can promote ice nucleation in small droplets of water or seawater (Knopf et al., 2011; Wilson et al., 2015; Ickes et al., 2020; Xi et al., 2021). Thus, diatoms like *F. cylindrus* may affect ice nucleation in cloud droplets.

There are some differences regarding the relevance of INPs in the Arctic and Antarctic polar regions. While in both polar latitudes the absolute concentrations of INPs are low, the influence of anthropogenic aerosols and INPs is much larger in the Arctic due to long-range transport during the Arctic winter (Šantl-Temkiv et al., 2019, 2020; Ekman and Schmale, 2022). During the Arctic summer, aerosol lifetimes are shorter due to increased wet removal preventing long-range transport and thus increasing the importance of locally

emitted INPs (Ekman and Schmale, 2022). In the Antarctic, the influence of anthropogenic aerosols and INPs is generally much smaller (Stohl and Sodemann, 2010; Ekman and Schmale, 2022). During winter, blowing snow from the sea ice is the main aerosol source in the southern polar region, while dimethyl sulfide and other organic compounds from algae blooms are the main source during summer (Ekman and Schmale, 2022).

In the following, we present experimental data on the ice nucleation activity of *F. cylindrus* diatom cells and their exudates. We then analyse and convert these data into a quantifiable format so that they can be compared to other measurements of this type. Finally, we provide a comparison to ice nucleation data of other polar diatoms together with a parameterization that generalizes their ice nucleation activity for use in atmospheric models.

2 Material and methods

2.1 Sampling and cultivation of the *F. cylindrus* diatoms

The investigated *F. cylindrus* cells belong to the strain TM99 isolated in 1999 from the sea ice of the Weddell Sea, Antarctica, by Thomas Mock (RV *Polarstern* ANT-XVI/3 expedition, which took place in the early spring from March to May 1999). Since then, stock cultures have been kept in $f/2$ medium (Guillard and Ryther, 1962) set up with Antarctic water and cultivated at 0 °C and under continuous illumination of approximately 25 µE m^{-2} s^{-1}. Before the experiment, cell numbers of the *F. cylindrus* cultures were monitored using a Coulter counter, and cells were harvested during the exponential growth phase. Cell cultures were distributed in 50 mL Falcon tubes, each containing about 1×10^8 cells, and they were centrifuged at 0 °C at 3220 g for 30 min. The clear spent $f/2$ medium was carefully separated from the cell pellet by pipetting, and both were shock-frozen in liquid nitrogen and stored at −80 °C.

2.2 Sample preparation

2.2.1 Preparation of artificial seawater

For the ice nucleation experiments, we used artificial seawater that mimics the natural conditions in the habitat of Antarctic *F. cylindrus* diatoms. The salinity in the Antarctic region is about 34.5, which corresponds to 34.5 g salts dissolved in 1000 g seawater (Roy-Barman and Jeandel, 2016), and we prepared artificial seawater of this salinity for dispersing the diatoms and as a reference for the ice nucleation experiments. To prepare the seawater, the six most important ions were considered, i.e. the cations sodium, potassium, magnesium, and calcium and the anions chloride and sulfate, which together make up about 99.4 % of the dissolved ions in seawater (Roy-Barman and Jeandel, 2016). The composition of the salts and their concentrations are given in Table S1 in the Supplement. The artificial seawater was filtered through a syringe filter (0.22 µm; polyethersulfone; SimplePure) in order to exclude any effect of suspended dust particles on ice nucleation. This filter has been used for all filtrations in this study, unless otherwise mentioned. The samples were stored at a temperature of −18 °C before use.

2.2.2 Preparation of *F. cylindrus* samples

The initial *F. cylindrus* samples contained about 10^8 diatoms per tube (see Sect. 2.1). These samples were placed in a micro-reaction tube and were filled up with the filtered artificial seawater to a volume of 2 mL. The resulting stock suspension of 5×10^7 cells per millilitre was used in all experiments. By further dilution with filtered artificial seawater, we generated several more dilute suspensions with concentrations of 1×10^7, 2×10^6, 1×10^6, and 5×10^5 cells per millilitre. For ice nucleation experiments on the fragments and exudates of the *F. cylindrus* cells, we filtered these five samples.

In order to identify the ice nucleating entities of the *F. cylindrus* samples, we separated the different components by means of filtration and centrifugation. We filtered a 1×10^7 cells per millilitre *F. cylindrus* suspension, such that the *F. cylindrus* cells should remain in the filter, while smaller fragments of destroyed cells and any soluble species, such as soluble ice-binding protein *fc*IBP11, should be able to pass the filter (see Fig. S1 in the Supplement for details). Thereafter, we recovered the filter cake containing the whole *F. cylindrus* cells and larger cell fragments by shaking the filter in a vial with artificial seawater. Although we used the same volume of artificial seawater as for the preparation of the original cell suspension, we surmise that the concentration of the resuspended diatoms is lower than the initial concentration. From the comparison of the frozen fraction curves obtained with the sample with those of unfiltered samples (see below), our best estimate of the concentration is about 2×10^6 cells per millilitre (estimated uncertainty range 1×10^6–1×10^7 cells per millilitre). Finally, the cell suspension was filtered again for comparison with the pure artificial seawater sample. To verify the method, all steps were also done with a vial of pure artificial seawater without suspended *F. cylindrus* cells.

We also performed ice nucleation experiments on fresh $f/2$ medium (Guillard and Ryther, 1962) and on the spent $f/2$ medium in which the *F. cylindrus* diatoms were actually grown. The sample preparation procedure is described in detail in Fig. S2. The spent $f/2$ medium should not contain many cells because they were separated by centrifugation. Nevertheless, we filtered the medium, such that only small fragments and soluble proteins (e.g. *fc*IBP11) should have remained in the filtrate (Bayer-Giraldi et al., 2011). In the next step, this sample was centrifuged using a 100 kDa centrifugal filter (polyethersulfone; Sartorius Vivaspin 500;

15 000 g), such that the remaining solution should not contain any diatom fragments but only smaller soluble molecules such as the soluble *fc*IBP11 protein. For comparison, we also applied the identical centrifugation step with a freshly prepared $f/2$ medium that had never been in contact with any diatoms.

2.2.3 Preparation of *P. syringae* samples

In additional experiments, we verified our Poisson evaluation procedure (see Sect. 2.3.3). For this purpose, we used well-studied bacterial cells of *P. syringae*, commercially available as Snomax®, from the same batch as that investigated in previous studies (Budke and Koop, 2015; Wex et al., 2015). The molecular mass of the individual ice nucleating proteins in the bacteria is about 150 kDa (Wolber et al., 1986; Govindarajan and Lindow, 1988). A suspension of *P. syringae*, with a concentration of $4\,\mathrm{mg\,mL^{-1}}$, was prepared from dry Snomax® with double-distilled water. By diluting this stock suspension with further double-distilled water, we also prepared additional, more dilute suspensions with concentrations of 1×10^{-2}, 2×10^{-3}, and $1 \times 10^{-3}\,\mathrm{mg\,mL^{-1}}$. Using an average value of the cell number density of 1.4×10^{9} cells per milligram (Wex et al., 2015), these mass concentrations correspond to cell concentrations of 1.4×10^{7}, 2.8×10^{6}, and 1.4×10^{6} cells per millilitre.

2.2.4 Preparation of *fc*IBP11

Previous studies suggest that *fc*IBP11 plays a major role in the response of *F. cylindrus* to freezing conditions (Bayer-Giraldi et al., 2010) by binding to the ice and affecting ice crystal growth (Bayer-Giraldi et al., 2011, 2018). For our experiments, we used the recombinant *fc*IBP isoform 11 (European Molecular Biology Laboratory, Heidelberg; GenBank accession no. DR026070). The protein was expressed, as previously described (Bayer-Giraldi et al., 2011), and resuspended in a Tris-HCl buffer (pH 7.0). To determine the ice nucleation activity of *fc*IBP11, we prepared a stock solution with a *fc*IBP11 concentration of $0.1\,\mathrm{mmol\,L^{-1}}$. We diluted this sample by a factor of 10 to a concentration of $0.01\,\mathrm{mmol\,L^{-1}}$, using a Tris-HCl buffer (pH 7.0), and performed ice nucleation experiments on both sample solutions with the modified WISDOM (WeIzmann Supercooled Droplets Observation on a Microarray) microfluidic experiment (Reicher et al., 2018; Eickhoff et al., 2019; see below).

2.3 Experimental methods for ice nucleation experiments

2.3.1 Differential scanning calorimetry

A classic method for the investigation of homogeneous and heterogeneous ice nucleation is differential scanning calorimetry (DSC) of emulsified droplets (Rasmussen and MacKenzie, 1972; Koop, 2004). Here, we used a DSC apparatus (TA Instruments; DSC Q100), which was described in detail previously, including its calibration procedure (Riechers et al., 2013). As bulk samples notoriously suffer from unwanted impurities, we performed measurements of inverse water-in-oil emulsion samples containing micrometre-sized droplets. As many thousands of droplets are investigated simultaneously, such samples allow the detection of very reproducible exothermic heterogeneous ice nucleation signals down to the homogeneous ice nucleation temperature of about −38 °C (Pinti et al., 2012; Riechers et al., 2013; Dreischmeier et al., 2017). Further information on the emulsion preparation procedure is given in the Supplement.

The DSC experiment has been used as a simple and direct method to check whether *F. cylindrus* diatoms are potential ice nucleators or not. The method does not allow for the observation of single droplets, and we can only study cell fragments, but not intact cells, because the latter are disrupted during the emulsion preparation process. Therefore, we have used the WISDOM microfluidic device, which is described below, as the main experimental method in this study.

2.3.2 WISDOM microfluidic device

Most of the ice nucleation experiments presented in this study were carried out using droplet microfluidics. In particular, we used a microfluidic device based upon the WISDOM experiment (Reicher et al., 2018, 2019), with some minor modifications for a set-up operated at Bielefeld University, including adapted temperature and heating rate calibrations (see a previous, detailed description; Eickhoff et al., 2019). These modifications and the general procedure for the sample preparation are given in the Supplement.

2.3.3 Evaluation procedure for samples with small INP concentrations

Ice nucleation studies using larger-volume droplet arrays usually employ relatively high concentrations of INPs per droplet, e.g. mineral dust particles or bacterial cells (Budke and Koop, 2015; Hiranuma et al., 2015, 2019; Wex et al., 2015; DeMott et al., 2018; Kunert et al., 2019; Ickes et al., 2020) to ensure that freezing is induced at a temperature that is higher than that triggered by the supporting surface or minute numbers of impurities contained in the water. In the present study, the total number of INPs was small due to the limited availability of *F. cylindrus* cells, suggesting the use of small droplet methods which require less total INP material. We investigated droplets with a diameter of 90 µm, corresponding to a volume of about 380 pL. Another, probably more important, advantage of using these small droplet volumes is that we can measure ice nucleation down to the homogenous freezing temperature of water (Riechers et al., 2013; Reicher et al., 2018; Tarn et al., 2021), also enabling the investigation of rather poor ice nucleators. As the concentrations c of *F. cylindrus* cells varied between 5×10^{5} and

5×10^7 cells per millilitre, the corresponding average INP concentrations ranged between 0.19 and 19 diatom cells per droplet. It becomes immediately clear that, when the average INP concentration λ is smaller than 1, i.e. on average less than one cell per droplet, there must be droplets devoid of any cells because the number of cells in an individual droplet can only be an integer (assuming only whole cells – without fragments – are present). In such a case, heterogeneous ice nucleation cannot be triggered in every droplet but only in those containing at least one cell. Hence, homogeneous ice nucleation is expected to occur in the empty droplets. Moreover, even if the average INP concentration λ is exactly one per droplet, there will be a few droplets that contain two or more INPs and, thus, other droplets that do not contain any INPs. The distribution of INPs among microfluidic droplets at small average INP concentration can be described using Poisson statistics (Huebner et al., 2007; Köster et al., 2008; Edd et al., 2009; Collins et al., 2015). The detailed documentation of this procedure is given in the Supplement.

2.4 Elemental analysis

The total carbon content of the *F. cylindrus* samples has been determined using elemental analysis. For this purpose, an amount of 0.7 mg *F. cylindrus* diatoms was combusted at a high temperature ($T > 1000\,^{\circ}\mathrm{C}$) in a tin crucible, and the composition was analysed using a commercially available elemental analyser (EuroVector, Euro EA Elemental Analyzer).

3 Results

3.1 Ice nucleation of *F. cylindrus*

Initially, the ice nucleation activity of *F. cylindrus* diatom cells was studied by differential scanning calorimetry (DSC). We found that fragments or exudates of *F. cylindrus* diatoms are potential ice nucleators, as the sample containing *F. cylindrus* diatoms induces freezing. The results are described in detail in the Supplement and in Fig. S8. These experiments initiated a more detailed study using the WISDOM microfluidic device. First, we investigated the ice nucleating properties of samples containing *F. cylindrus* diatom cells, in addition to fragments and exudates, at different concentrations suspended in artificial seawater. We used the droplet microfluidic device described in Sect. 2.3.2 above. The results of these experiments are presented in Fig. 2a, which shows, as a function of temperature, the frozen fraction of droplets f_{ice}, commonly defined as the cumulative number of droplets frozen when cooled to a certain temperature relative to the total number of droplets (Murray et al., 2012). Thus, f_{ice} is practically independent of the total number of droplets investigated in a particular experiment. In our case, the number of droplets varied between 45 and 70 droplets per single measurement, and typically three single measurements per sample were performed. Figure 2a shows that the freezing temperatures of all *F. cylindrus* samples (coloured symbols) are higher than that of the artificial seawater reference sample (grey symbols), hence supporting the observations from the DSC experiments that the *F. cylindrus* diatoms promote ice nucleation. To compare the different samples, we use the T_{50} temperature, which is the temperature at which half of the observed droplets are frozen, i.e. $f_{\mathrm{ice}} = 0.5$. For the artificial seawater, we measured a T_{50} of $-40.1\,^{\circ}\mathrm{C}$, and T_{50} of the *F. cylindrus* suspensions shifted to a higher temperature by between about 2.8 and 7.2 °C with increasing diatom concentration. Detailed information on the increase in T_{50} of the different concentrations is given in Table S4. This significant concentration dependence of the T_{50} shift reveals that not all diatoms nucleate ice at the same temperature, and this implies a distribution of the ice nucleation efficiency as has been observed previously also for other ice nucleators (Herbert et al., 2014; Budke and Koop, 2015).

This is visualized better by plotting the cumulative number n_N of ice nucleating sites per number of *F. cylindrus* diatom cells, defined in Eq. (S9), as a function of freezing temperature (see Fig. 3). This n_N value is independent of the concentration of investigated INP and of the size of the investigated droplets but can be measured for a wide range of temperatures, using different concentrations, and allows for the comparison with results from other experimental techniques (see the discussion below). Figure 3 reveals that, at $-30.0\,^{\circ}\mathrm{C}$, $\sim 0.1\,\%$ of the *F. cylindrus* diatom cells promote ice nucleation, which increases to $\sim 1\,\%$ at $-32.0\,^{\circ}\mathrm{C}$ and $\sim 10\,\%$ at $-33.5\,^{\circ}\mathrm{C}$. Between about -35.0 and $-36.5\,^{\circ}\mathrm{C}$ all *F. cylindrus* cells trigger the nucleation of ice, i.e. $n_N = 1$. By definition, n_N values larger than 1 should not be possible because it would imply that one diatom can induce the freezing of more than one droplet, which is unreasonable. The highest n_N values occur at the lowest diatom concentrations, and therefore, we must consider Poisson statistics, i.e. whether or not each droplet indeed contains a diatom cell. Following the treatise mentioned in Sect. 2.3.3 and outlined in detail in the Supplement and using Eq. (S7), in Fig. 3 we indicate all the droplets that contain at least one diatom as filled circles, while all droplets that do not contain any *F. cylindrus* diatom cells are displayed as open circles. This analysis reveals a relatively sharp transition between filled and unfilled circles at n_N values of about one ice nucleating active site per diatom cell. All droplets frozen at $n_N 1$ (and lower temperatures) do not contain intact *F. cylindrus* cells. We suggest that their freezing is induced by cell fragments or by INPs released by the *F. cylindrus* diatoms, e.g. soluble species from the EPSs such as proteins or polysaccharides. A similar behaviour has been observed previously for birch pollen that releases about 10^4 ice nucleators per pollen particle, which turned out to be ice nucleating macromolecules (Pummer et al., 2012, 2015; Augustin et al., 2013; Dreischmeier et al., 2017).

To verify the above interpretation, we performed experiments in which the samples from the measurements shown in

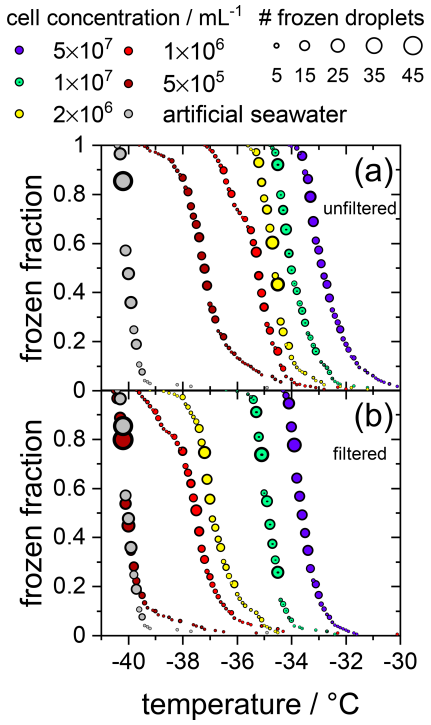

Figure 2. Cumulative fraction of frozen droplets as a function of temperature for different *F. cylindrus* cell concentrations (coloured circles) and pure artificial seawater (grey circles) as a reference. The size of the circles indicates the number of droplets frozen within the same temperature interval (0.1 °C). Every data set combines three individual measurements each containing between 45 and 70 droplets. **(a)** Frozen fraction curves for the five *F. cylindrus* samples, containing mostly whole diatoms and, probably, some fragments. **(b)** Freezing temperatures of the filtered (0.22 µm) samples. These samples, thus, contain no whole cells but fragments, in addition to proteins and other soluble components. Note that the concentrations refer to the diatom concentrations before filtration. The seawater reference (grey circles) is the same in both panels.

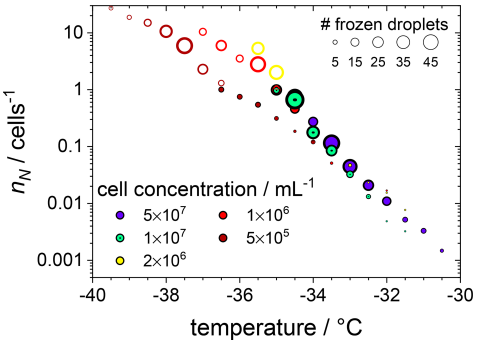

Figure 3. The cumulative number of ice nucleating sites n_N per number of *F. cylindrus* diatom cells as a function of temperature, obtained from the data shown in Fig. 2a with the help of Eq. (S9). The original data were binned into intervals of 0.5 °C. The size of the symbols indicates the absolute number of droplets frozen in a particular bin, and the cell concentrations (in mL^{-1}) are indicated by colour. The filled circles represent the droplets that contain whole *F. cylindrus* cells, while Poisson statistics suggest that the open circles should not contain any intact diatoms but probably some cell fragments (see text).

Figs. 2a and 3 were filtered with a pore size of 0.22 µm. This procedure removes intact whole diatoms, which are about 4.5 to 74 µm for the apical axis and 2.4 to 4 µm for the transapical axis (Lundholm and Hasle, 2008; Cefarelli et al., 2010). In Fig. 2b, the cumulative fraction of frozen droplets of these filtered samples is shown. The symbol colours represent the same suspensions as shown in Fig. 2a, but filtered, and the artificial seawater reference data are identical to that in Fig. 2a. All frozen fraction curves are shifted to lower temperatures when compared to the unfiltered samples, suggesting a significant, but not entire, removal of INPs. Only the filtrate of the suspension with the lowest concentrations reveals a T_{50} that is the same as the seawater reference (−40.1 °C), suggesting that this sample does not contain any significant concentration of INPs after filtration. All other filtrated suspensions show T_{50} values that are higher by between 2.6 and 6.4 °C relative to the seawater. For further information on the T_{50} shifts, see Table S4. Together, these results imply that either fragments of *F. cylindrus* or molecules released by the diatoms can nucleate ice but with a significantly reduced efficiency than intact diatoms. Moreover, these results can also explain the observations in Fig. 3 of ice nucleation of droplets at $n_N 1$ that do not contain any full diatom cells. Below, we present further experiments to investigate the nature of the ice-nucleating particles.

3.2 Ice nucleation of resuspended *F. cylindrus* cells

In the following experiments, we separated diatom cells from their fragments or released INPs. For this purpose, the sample suspension of *F. cylindrus* with a concentration of 1×10^7 cells per millilitre, which was shown already in Fig. 2, was analysed further, and the results are presented in Fig. 4. The green data points are those of the unfiltered sample, which is identical to that shown in Fig. 2a, and the magenta data points are identical to the filtered solution already presented in Fig. 2b (shown there as green data points). This suspension should contain only INPs smaller than 0.22 µm. Next, most (but not all) of the diatom cells and fragments contained in the filter cake of that filtration procedure were resuspended in artificial seawater. Thus, the concentration of the resuspended cells is about 2×10^6 cells per millilitre (estimated uncertainty range 1×10^6–1×10^7 cells per millilitre). The frozen fraction of that sample is shown as the orange data points in Fig. 4 and shows the same ice nucleation onset temperature of about −32.5 °C as the original unfiltered suspension (green). However, the curve is broader, suggesting that it contains less of the most active ice nucleators. To verify that all fragments smaller than 0.22 µm had been leached

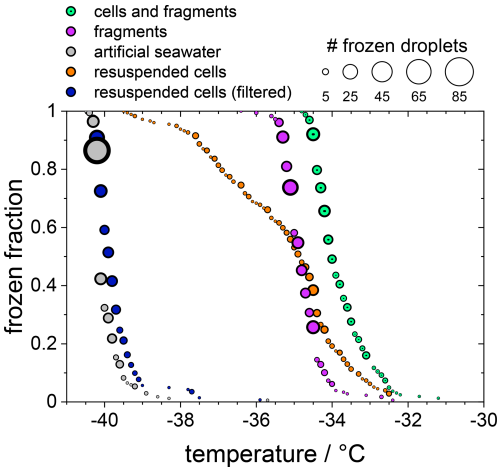

Figure 4. The frozen fraction of a sample with 1×10^7 *F. cylindrus* diatoms per millilitre after different treatments. The symbol size indicates the total number of droplets frozen at that temperature. The green coloured data are the untreated sample and are the same as those in Fig. 2a. The magenta data are the filtered sample that should just contain fragments of the diatoms. These are the same data as the green data in Fig. 2b. The grey data points show the freezing of the artificial seawater for reference (also replotted from Fig. 2). The orange data show the freezing of the diatoms that were resuspended from the filter into artificial seawater. Its concentration is likely smaller than 1×10^7 cells per millilitre because not all cells could be resuspended. The blue data points represent the freezing of the droplets consisting of the resuspended cell suspension after renewed filtration; it should not contain any diatoms or fragments.

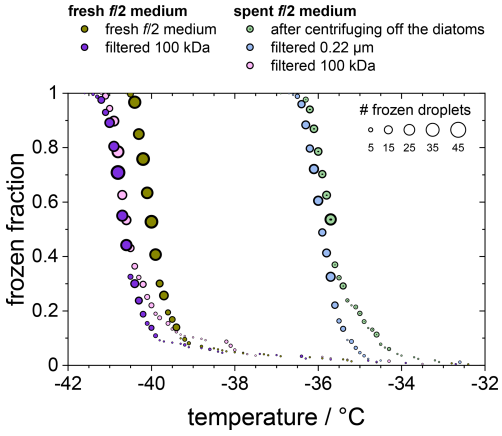

Figure 5. Frozen fraction of differently treated $f/2$ nutria media as a function of temperature. The olive and purple circles belong to a fresh $f/2$ medium that is untreated (olive) or had been filtered using a 100 kDa filter (purple). The green, blue, and pink circles belong to the untreated, 0.22 µm filtered, and 100 kDa filtered spent medium in which the *F. cylindrus* diatoms had grown before they were centrifuged and separated from the medium.

out during the first filtration step, this resuspended filter cake sample was filtered again with a 0.22 µm filter. The results of this procedure on the freezing behaviour are shown as the blue circles in Fig. 4. The frozen fraction data are practically identical to that of the artificial seawater, suggesting that the filtration of the pure whole cells has been successful, and hardly any fragments smaller than 0.22 µm are left in the filtrate. This analysis also implies that the ice nucleation of the unfiltered suspension is due to whole cells and cell fragments but not due to ice nucleating molecules released from the diatoms. The T_{50} shift upon filtration of about 1.5 °C is similar in magnitude to the effect of reducing the concentration of the unfiltered diatoms from 5×10^7 to 1×10^7 cells per millilitre, i.e. by a factor of 5. This similarity may indicate that fragments make up about 10 %–20 % of the INPs in the unfiltered samples, which agrees with the fact that some ice nucleation is observed for values of $n_N 1$ (see Fig. 3).

3.3 Ice nucleation of spent medium and of purified *fc*IBP11

We also investigated the spent $f/2$ medium (Guillard and Ryther, 1962), i.e. the medium in which the *F. cylindrus* diatoms were cultivated before they were separated by centrifugation to investigate their ice nucleating effects. Separation of the diatoms from the spent $f/2$ medium by centrifugation is not perfect, and hence, smaller fragments, in addition to soluble macromolecules such as proteins, may remain in the spent medium. These may be potential ice nucleators, as it has been shown previously that even smaller ice-binding antifreeze proteins can act as ice nucleators at lower temperatures (Eickhoff et al., 2019).

In Fig. 5 we compare the frozen fraction curve for the spent $f/2$ medium (light green circles) with that of a freshly prepared $f/2$ medium, which had never been in contact with any *F. cylindrus* diatoms (olive circles). Clearly, the spent medium, even after centrifuging off the diatoms, shows significant ice nucleation with a T_{50} of about −35.7 °C, while the T_{50} of the fresh medium is much lower at −40.0 °C. In additional experiments, the spent medium has been filtered in two further steps, first by using a 0.22 µm syringe filter (light blue circles) and then by using a 100 kDa centrifugation filter (pink circles). For comparison, the fresh medium has been also filtered with a 100 kDa centrifugation filter (purple circles). Obviously, filtration of the spent medium with a 0.22 µm filter shows hardly any effect on ice nucleation, as its T_{50} is shifted to −36.0 °C, which is the same as the unfiltered sample within the temperature uncertainty in our set-up of ±0.3 °C.

In contrast, filtration with a 100 kDa filter substantially reduced the ice nucleation with a T_{50} value of −40.6 °C, which is the same as that of the filtrated fresh medium of −40.7 °C, suggesting that the 100 kDa filter removed all remaining ice nucleators present in the spent medium. This observation suggests that any macromolecules smaller than 100 kDa that were present in the spent medium are not ice nucleation active because otherwise they would have passed the

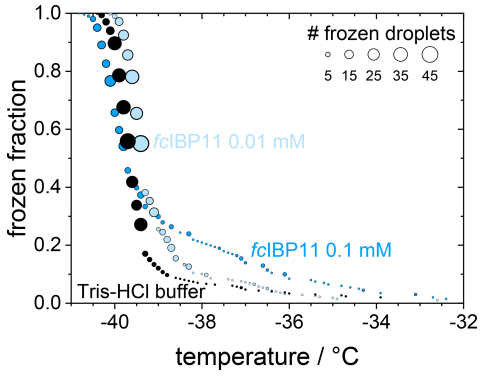

Figure 6. Cumulative frozen fractions as a function of temperature of droplets containing *fc*IBP11 solutions with concentrations of 0.1 mmol L^{-1} (dark blue) and 0.01 mmol L^{-1} (light blue). The black circles show the freezing of the Tris-HCl buffer for reference. The circle area indicates the number of droplets frozen at a particular temperature.

filter and led to an increased T_{50} when compared to the fresh medium. The ice-binding proteins present in and/or released from *F. cylindrus* are similar in size to the well-characterized *fc*IBP11, which is about 26 kDa (Bayer-Giraldi et al., 2011). Thus, ice-binding proteins released by the *F. cylindrus* into the spent medium should have passed the filter and could have induced ice nucleation if they had significant ice nucleation activity. However, the results shown in Fig. 5 do not reveal any ice nucleation activity. This may be interpreted as follows. Either the proteins remaining in the filtrate do not promote ice nucleation or *F. cylindrus* does not release any proteins into the spent medium. To shed further light on the ice nucleating ability of ice-binding proteins from *F. cylindrus*, we studied purified *fc*IBP11 samples in additional experiments. We studied the ice nucleation activity of two *fc*IBP11 solutions of different concentrations and that of the pure Tris-HCl buffer for comparison. The results are presented in Fig. 6. The two *fc*IBP11 samples with 0.1 mM (dark blue circles) and 0.01 mM (light blue circles) concentrations reveal T_{50} values of −39.8 and −39.4 °C, which are equal to the $T_{50} = 39.7$ °C of the buffer reference (black circles) within experimental temperature uncertainty (±0.3 °C). Thus, no significant shift in the freezing temperature is observed, and even when considering the increased ice nucleation temperature of the *fc*IBP11 at frozen fractions below about 25 %, it appears that *fc*IBP11 is not an efficient ice nucleator with relevance for atmospheric or biospheric processes, owing to its unnaturally high concentration in the droplet samples investigated here. These observations agree with recent theoretical studies, which suggest that moderate antifreeze IBPs show no nucleation of ice perpendicular to the basal and prismatic ice planes (Cui et al., 2022). And indeed, the basal and prismatic planes are exactly those planes at which the moderate *fc*IBP11 binds to ice (Kondo et al., 2018).

Overall, the results show that *F. cylindrus* diatom cells and cell fragments suspended in seawater can induce heterogeneous ice nucleation, while ice-binding proteins produced by *F. cylindrus*, such as *fc*IBP11, have negligible ice nucleation activity.

4 Discussion and implications

Here, we put the above results in the context of previous ice nucleation studies on diatoms. Triggered by the pioneering initial laboratory studies of marine-diatom-induced ice nucleation (Alpert et al., 2011; Knopf et al., 2011), modelling studies have shown that, in some regions of the atmosphere, marine diatoms may contribute to the atmospheric INP (Burrows et al., 2013; Ickes et al., 2020). To use laboratory ice nucleation data in such models, the data must be evaluated and parameterized appropriately. For example, a direct comparison of T_{50} or f_{ice} originating from different laboratory studies on different types of INPs is not meaningful, as different sample volumes, INP concentrations, buffer concentrations, etc., may have been used. Therefore, it is preferable to compare the cumulative number of ice nucleating active sites per mass, surface area, or the number of the INPs. Here, we make a comparison based on total INP mass, using the following definition of the cumulative number of ice nucleating active sites per mass n_{m_total} (Murray et al., 2012; Hiranuma et al., 2015, 2019; Xi et al., 2021).

$$n_{m\_total} = \frac{-\ln(1 - f_{ice})}{c_{m\_total} \cdot V}. \quad (1)$$

Here, V is the volume of an individual droplet in the experiment, and c_{m_total} is the total mass of biological material per droplet. For the *F. cylindrus* samples investigated here, we used the total carbon mass per *F. cylindrus* cell from the literature (Kang and Fryxell, 1992) and performed elemental analysis to obtain the carbon content of our samples, resulting in a value of 39.32 % to calculate the average total mass per individual *F. cylindrus* diatom cell of $m_{total} = 4.5 \times 10^{-11}$ g. Using these values and our experimental data in Eq. (1), we have calculated the ice nucleating active sites n_{m_total} of the *F. cylindrus* diatoms (see the blue circles in Fig. 7). We have fitted this data set and provide a corresponding parameterization (see Fig. S9 and Eq. S10.) Also shown in Fig. 7 are n_{m_total} data of the sea ice diatoms *Melosira arctica* (blue squares) and *Nitzschia stellata* (blue triangles) and of the temperate diatom *Skeletonema marinoi* (open orange circles) from previous studies (Ickes et al., 2020; Xi et al., 2021).

To allow a direct comparison of ice nucleation of the different diatoms, which were studied in different types of aqueous solutions, all the ice nucleation temperatures shown in Fig. 7 have been corrected (either by the original authors or by us) for the colligative solute effect and represent diatom ice nucleation in pure water. We have corrected the freezing

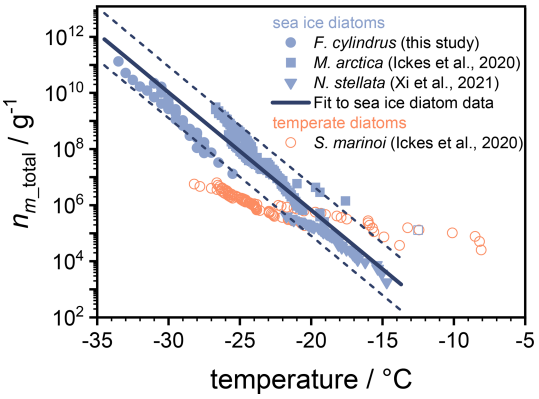

Figure 7. Experimental data of $n_{\mathrm{m\_total}}$, i.e. the number of ice active sites per total mass of *F. cylindrus* diatom cells (blue circles) and other sea ice diatoms (blue squares and triangles) from previous studies, in addition to $n_{\mathrm{m\_total}}$ data for one temperate diatom species (open orange circles; Ickes et al., 2020; Xi et al., 2021). The solid line represents a fit of the $n_{\mathrm{m\_total}}$ values for the three sea ice diatom species (see Eq. 2), while the dashed lines indicate the 2σ upper and lower prediction bands of this fit. All temperatures were corrected for the freezing point depressions of different buffers and solutes, so that they represent the ice nucleation induced by the diatoms in pure water. The $n_{\mathrm{m\_total}}$ values for *N. stellata* were provided by the authors (Xi et al., 2021). For *M. arctica* and the *S. marinoi*, we calculated $n_{\mathrm{m\_total}}$ from the total number of cells given in the original work and provided by the authors (Ickes et al., 2020) and assume cell volumes of 653 and 125 µm^3 and a cell density of 1 mg mL^{-1} (Olenina et al., 2006; Xi et al., 2021).

temperatures of the *F. cylindrus* samples by the measured difference between the T_{50} of pure double-distilled water and pure artificial seawater without any diatoms.

The comparison in Fig. 7 reveals that the curves of the three sea ice diatoms complement one another, as $n_{\mathrm{m\_total}}$ values of different magnitudes have been obtained over different temperature ranges. Interestingly, while some offsets exist between the different data sets, their slopes are quite similar. In contrast, the slope of the $n_{\mathrm{m\_total}}$ data of the temperate diatom is significantly smaller. The observed similarities of the sea ice diatom data sets suggest a more generalized description of their behaviour in models. For this purpose, we fitted these data sets to provide a parametrization of $n_{\mathrm{m\_total}}$ as a function of temperature. The three different data sets consist of different numbers of data points which were taken into account in order to give each data set the same statistical weight. We further note that one strongly deviating data point from the *M. arctica* data set (indicated as an open square in Fig. 7) was excluded from the fitting procedure. The resulting parameterization is given as follows:

$$\log_{10}(n_{\mathrm{m\_total}}\,\mathrm{g}^{-1}) = -0.420053\,^{\circ}\mathrm{C}^{-1} \cdot T - 2.57818, \qquad (2)$$

where T is temperature to be entered in units of degrees Celsius. For numerical code verification, Eq. (2) should result in a value for $n_{\mathrm{m\_total}}$ of 6.7×10^5 g^{-1} at a temperature of −20.0 °C. This parameterization is valid over the temperature range between −13.7 and −34.5 °C. The parameterization is shown as the thick solid line in Fig. 7, and the upper and lower 2σ prediction bands are given as dashed lines. In summary, Fig. 7 shows that the parameterization line and its prediction bands are an appropriate representation of the ice nucleation activity of three types of sea ice diatoms suitable for use in atmospheric or biogeosciences model applications.

In the following, we put the ice nucleation data of *F. cylindrus* and the other sea ice diatoms into context by comparing to field studies. Wilson et al. (2015) provided experimental evidence for a marine biogenic source of ice nucleating particles and suggested that exudates and fragments of diatoms as a source of the ice nucleating material located in the sea surface microlayer. Their low-temperature freezing data reveal a cumulative number of ice nucleating active sites per total organic carbon mass $n_{\mathrm{m\_TOC}}$ of $\sim 1.3 \times 10^{10}$ g^{-1} at −27 °C (calculated from the equation given in the caption of their Fig. 2), which is the low-temperature end of their data, and the most relevant to the present study. To compare this value to the $n_{\mathrm{m\_total}}$ values given in Fig. 7, we estimated that the organic carbon content of their samples varies between 39.32 % (representing the organic carbon content of *F. cylindrus* cells; see above) or 100 % (representing a purely organic carbon composition), resulting in a range of $n_{\mathrm{m\_total}}$ of $\sim 5.0 \times 10^9$–1.3×10^{10} g^{-1} for their Arctic sea surface microlayer samples. These are compared to $n_{\mathrm{m\_total}}$ values of 8.2×10^7 g^{-1} (2σ prediction bands of 2.8×10^7–2.4×10^8 g^{-1}) for *F cylindrus* and of 5.8×10^8 g^{-1} (2σ prediction bands of 7.0×10^7–4.8×10^9 g^{-1}) for sea ice diatoms, respectively, at −27 °C, indicating that *F. cylindrus* and other sea ice diatoms may contribute to the marine INP in the Southern Ocean and Antarctic seawater, assuming the Wilson et al. (2015) parameterization also applies to these areas.

In another comparison, we use measurements of insoluble aerosol particles made at Amsterdam Island in the southern Indian Ocean (Gaudichet et al., 1989). These measurements show that marine biogenic particles make up between 8 % and 28 % of the number of detected particles and that these were predominantly assigned to *Radiolaria* and diatom fragments (identified as amorphous silicates), with about 27 % or 2.7×10^4 m^{-3} particles observed in the southern winter (July) and fewer in fall (May; 8 %; 2.4×10^4 m^{-3}) and spring (September; 7 %; 1.8×10^3 m^{-3}). If we assume that all *Radiolaria* and diatom fragments can be attributed to *F. cylindrus* diatoms, we can calculate the mass concentration of *F. cylindrus* diatom cells per cubic metre of air from the mass of an individual cell ($m_{\mathrm{total}} = 4.5 \times 10^{-11}$ g; see above), yielding values of 1.2×10^{-6} g m^{-3} of air (July), 1.1×10^{-6} g m^{-3} of air (May), and 8.1×10^{-8} g m^{-3} of air (September). Using the parametrization of the cumulative number of ice nucleating active sites per mass *F. cylindrus* in Eq. (S10), we calculate a $n_{\mathrm{m\_total}}$ value of 8.2×10^7 g^{-1} (2σ prediction bands are 2.8×10^7–2.4×10^8 g^{-1}) at −27 °C (see above), from which we can derive the ~ 88 INP m^{-3} air (2σ of 3–250) at −27 °C

in fall (May). This value can be compared to in situ total INP measurements in the Southern Ocean south of Australia in fall (March–April), yielding values between 34 and 207 INPs per cubic metre of air at −27 °C (McCluskey et al., 2018). Although the above calculations are order-of-magnitude estimates, the comparison shows that it is not unreasonable that sea ice diatoms such as *F. cylindrus*, and their fragments may constitute a significant fraction of the INP in the Southern Ocean and Antarctic waters.

5 Summary and conclusions

Cells and fragments of *F. cylindrus* diatoms can induce heterogeneous ice nucleation in artificial seawater by up to 7.2 °C higher temperature (for the largest concentration investigated, i.e. 5×10^7 cells per millilitre) than the homogeneous ice nucleation temperature in pure seawater. We also observed an ice nucleating effect of fragments smaller than 0.22 µm, in agreement with previous observations of the relevance of nanoscale biological fragments for ice nucleation (O'Sullivan et al., 2015; Wilson et al., 2015; Irish et al., 2017, 2019; Hartmann et al., 2021). For the ice-binding (antifreeze) protein *fc*IBP11, we did not observe any evidence for promoting ice nucleation at low temperatures. Using the information that *F. cylindrus* may serve as INPs, we can estimate their atmospheric relevance. Due to their smaller size and, thus, longer atmospheric residence time, especially fragments of diatoms are expected to be relevant for atmospheric ice nucleation because the atmospheric lifetime of entire *F. cylindrus* diatoms is estimated to be below 1 d due to deposition (Hobbs, 2000; Seinfeld and Pandis, 2016). There are only a few studies that describe the aerosolization and atmospheric transport processes of diatoms and diatom fragments in addition to their atmospheric detection at different altitudes (Brown et al., 1964; Gaudichet et al., 1989; Leck and Bigg, 2008; Burrows et al., 2013). Based on order-of-magnitude estimations comparing field observations of the Southern Ocean with our laboratory results, we suggest that diatoms like *F. cylindrus* and their fragments may contribute to ice nucleation in marine environments of the polar regions at low temperatures where sea ice diatoms become active for ice nucleation (Fig. 7). To improve these estimates, more observations of the atmospheric abundance of diatoms and INPs in general and in the Antarctic marine environments are required, and modelling studies of the sea-to-air transfer of diatoms and their fragments are needed. In this respect, we observed a common behaviour of the cumulative number of ice nucleating active sites per mass of diatom among three different types of sea ice diatoms. This similarity may originate from a similar biological function of the ice nucleation ability in sea ice diatoms, and a corresponding parameterization developed thereof may simplify the representation of their properties in atmospheric and biogeochemical models.

Data availability. The experimental data presented in the figures of this paper are provided in tabular form in the Supplement.

Supplement. The supplement related to this article is available online at: https://doi.org/10.5194/bg-20-1-2023-supplement.

Author contributions. LE and TK designed the study. MBG provided the protein samples, LE performed the calibration and both DSC and microfluidic ice nucleation experiments, and NR prepared the microfluidic devices. LE did the data analysis and the Poisson statistics calculations, with input from TK. LE and TK prepared the figures. LE, TK and MBG wrote the paper, with input from YR and NR. All authors contributed to the discussion of the data and text and approved the final version of the paper.

Competing interests. The contact author has declared that none of the authors has any competing interests.

Disclaimer. Publisher's note: Copernicus Publications remains neutral with regard to jurisdictional claims in published maps and institutional affiliations.

Acknowledgements. We thank Arika Allhusen and Klaus Valentin, for providing the original *F. cylindrus* samples, and Luisa Ickes, Yu Xi, and Allan Bertram, for provision of original data sets on diatom ice nucleation and for helpful comments.

Financial support. We acknowledge support for the publication costs by the open-access publication fund of Bielefeld University and the Deutsche Forschungsgemeinschaft (DFG). Maddalena Bayer-Giraldi is grateful for support from the Deutsche Forschungsgemeinschaft SPP1158 (German Research Association programme no 1158; grant no. BA 3694/2-1).

This open-access publication was funded by Bielefeld University.

Review statement. This paper was edited by Anja Engel and reviewed by Manuel Dall'Osto and one anonymous referee.

References

Ackley, S. F. and Sullivan, C. W.: Physical controls on the development and characteristics of Antarctic sea ice biological communities – a review and synthesis, Deep Sea Res. Pt. I, 41, 1583–1604, https://doi.org/10.1016/0967-0637(94)90062-0, 1994.

Alpert, P. A., Aller, J. Y., and Knopf, D. A.: Ice nucleation from aqueous NaCl droplets with and without marine diatoms, Atmos. Chem. Phys., 11, 5539–5555, https://doi.org/10.5194/acp-11-5539-2011, 2011.

Aslam, S. N., Strauss, J., Thomas, D. N., Mock, T., and Underwood, G. J. C.: Identifying metabolic pathways for production of extracellular polymeric substances by the diatom Fragilariopsis cylindrus inhabiting sea ice, ISME J., 12, 1237–1251, https://doi.org/10.1038/s41396-017-0039-z, 2018.

Aslam, S. N., Cresswell-Maynard, T., Thomas, D. N., and Underwood, G. J. C.: Production and Characterization of the Intra- and Extracellular Carbohydrates and Polymeric Substances (EPS) of Three Sea-Ice Diatom Species, and Evidence for a Cryoprotective Role for EPS, J. Phycol., 48, 1494–1509, https://doi.org/10.1111/jpy.12004, 2012a.

Aslam, S. N., Underwood, G. J. C., Kaartokallio, H., Norman, L., Autio, R., Fischer, M., Kuosa, H., Dieckmann, G. S., and Thomas, D. N.: Dissolved extracellular polymeric substances (dEPS) dynamics and bacterial growth during sea ice formation in an ice tank study, Polar. Biol., 35, 661–676, https://doi.org/10.1007/s00300-011-1112-0, 2012b.

Augustin, S., Wex, H., Niedermeier, D., Pummer, B., Grothe, H., Hartmann, S., Tomsche, L., Clauss, T., Voigtländer, J., Ignatius, K., and Stratmann, F.: Immersion freezing of birch pollen washing water, Atmos. Chem. Phys., 13, 10989–11003, https://doi.org/10.5194/acp-13-10989-2013, 2013.

Bar Dolev, M., Braslavsky, I., and Davies, P. L.: Ice-Binding Proteins and Their Function, Annu. Rev. Biochem., 85, 515–542, https://doi.org/10.1146/annurev-biochem-060815-014546, 2016.

Bartsch, A.: Sea Ice Algae of the Weddell Sea (Antarctica): Species Composition, Biomass, and Ecophysiology of Selected Species, Ber. Polarforsch., 63, p. 89, 1989.

Bayer-Giraldi, M., Uhlig, C., John, U., Mock, T., and Valentin, K.: Antifreeze proteins in polar sea ice diatoms: diversity and gene expression in the genus Fragilariopsis, Environ. Microbiol., 12, 1041–1052, https://doi.org/10.1111/j.1462-2920.2009.02149.x, 2010.

Bayer-Giraldi, M., Sazaki, G., Nagashima, K., Kipfstuhl, S., Vorontsov, D. A., and Furukawa, Y.: Growth suppression of ice crystal basal face in the presence of a moderate ice-binding protein does not confer hyperactivity, P. Natl. Acad. Sci. USA, 115, 7479–7484, https://doi.org/10.1073/pnas.1807461115, 2018.

Bayer-Giraldi, M., Weikusat, I., Besir, H., and Dieckmann, G.: Characterization of an antifreeze protein from the polar diatom Fragilariopsis cylindrus and its relevance in sea ice, Cryobiology, 63, 210–219, https://doi.org/10.1016/j.cryobiol.2011.08.006, 2011.

Brown, R. M., Larson, D. A., and Bold, H. C.: Airborne Algae: Their Abundance and Heterogeneity, Science (New York, N.Y.), 143, 583–585, https://doi.org/10.1126/science.143.3606.583, 1964.

Budke, C. and Koop, T.: BINARY: an optical freezing array for assessing temperature and time dependence of heterogeneous ice nucleation, Atmos. Meas. Tech., 8, 689–703, https://doi.org/10.5194/amt-8-689-2015, 2015.

Burrows, S. M., Hoose, C., Pöschl, U., and Lawrence, M. G.: Ice nuclei in marine air: biogenic particles or dust?, Atmos. Chem. Phys., 13, 245–267, https://doi.org/10.5194/acp-13-245-2013, 2013.

Cefarelli, A. O., Ferrario, M. E., Almandoz, G. O., Atencio, A. G., Akselman, R., and Vernet, M.: Diversity of the diatom genus Fragilariopsis in the Argentine Sea and Antarctic waters: morphology, distribution and abundance, Polar. Biol., 33, 1463–1484, https://doi.org/10.1007/s00300-010-0794-z, 2010.

Collins, D. J., Neild, A., deMello, A., Liu, A.-Q., and Ai, Y.: The Poisson distribution and beyond: methods for microfluidic droplet production and single cell encapsulation, Lab Chip, 15, 3439–3459, https://doi.org/10.1039/c5lc00614g, 2015.

Creamean, J. M., Hill, T. C. J., DeMott, P. J., Uetake, J., Kreidenweis, S., and Douglas, T. A.: Thawing permafrost: an overlooked source of seeds for Arctic cloud formation, Environ. Res. Lett., 15, 84022, https://doi.org/10.1088/1748-9326/ab87d3, 2020.

Creamean, J. M., Ceniceros, J. E., Newman, L., Pace, A. D., Hill, T. C. J., DeMott, P. J., and Rhodes, M. E.: Evaluating the potential for Haloarchaea to serve as ice nucleating particles, Biogeosciences, 18, 3751–3762, https://doi.org/10.5194/bg-18-3751-2021, 2021.

Cui, S., Zhang, W., Shao, X., and Cai, W.: Do Antifreeze Proteins Generally Possess the Potential to Promote Ice Growth?, Phys. Chem. Chem. Phys., 24, 7901–7908, https://doi.org/10.1039/D1CP05431G, 2022.

Davies, P. L.: Ice-binding proteins: a remarkable diversity of structures for stopping and starting ice growth, Trends Biochem. Sci., 39, 548–555, https://doi.org/10.1016/j.tibs.2014.09.005, 2014.

DeMott, P. J., Hill, T. C. J., McCluskey, C. S., Prather, K. A., Collins, D. B., Sullivan, R. C., Ruppel, M. J., Mason, R. H., Irish, V. E., Lee, T., Hwang, C. Y., Rhee, T. S., Snider, J. R., McMeeking, G. R., Dhaniyala, S., Lewis, E. R., Wentzell, J. J. B., Abbatt, J., Lee, C., Sultana, C. M., Ault, A. P., Axson, J. L., Diaz Martinez, M., Venero, I., Santos-Figueroa, G., Stokes, M. D., Deane, G. B., Mayol-Bracero, O. L., Grassian, V. H., Bertram, T. H., Bertram, A. K., Moffett, B. F., and Franc, G. D.: Sea spray aerosol as a unique source of ice nucleating particles, P. Natl. Acad. Sci. USA, 113, 5797–5803, https://doi.org/10.1073/pnas.1514034112, 2016.

DeMott, P. J., Möhler, O., Cziczo, D. J., Hiranuma, N., Petters, M. D., Petters, S. S., Belosi, F., Bingemer, H. G., Brooks, S. D., Budke, C., Burkert-Kohn, M., Collier, K. N., Danielczok, A., Eppers, O., Felgitsch, L., Garimella, S., Grothe, H., Herenz, P., Hill, T. C. J., Höhler, K., Kanji, Z. A., Kiselev, A., Koop, T., Kristensen, T. B., Krüger, K., Kulkarni, G., Levin, E. J. T., Murray, B. J., Nicosia, A., O'Sullivan, D., Peckhaus, A., Polen, M. J., Price, H. C., Reicher, N., Rothenberg, D. A., Rudich, Y., Santachiara, G., Schiebel, T., Schrod, J., Seifried, T. M., Stratmann, F., Sullivan, R. C., Suski, K. J., Szakáll, M., Taylor, H. P., Ullrich, R., Vergara-Temprado, J., Wagner, R., Whale, T. F., Weber, D., Welti, A., Wilson, T. W., Wolf, M. J., and Zenker, J.: The Fifth International Workshop on Ice Nucleation phase 2 (FIN-02): laboratory intercomparison of ice nucleation measurements, Atmos. Meas. Tech., 11, 6231–6257, https://doi.org/10.5194/amt-11-6231-2018, 2018.

Dreischmeier, K., Budke, C., Wiehemeier, L., Kottke, T., and Koop, T.: Boreal pollen contain ice-nucleating as well as ice-binding "antifreeze" polysaccharides, Sci. Rep., 7, 41890, https://doi.org/10.1038/srep41890, 2017.

Edd, J. F., Humphry, K. J., Irimia, D., Weitz, D. A., and Toner, M.: Nucleation and solidification in static arrays of monodisperse drops, Lab Chip, 9, 1859–1865, https://doi.org/10.1039/b821785h, 2009.

Eicken, H.: The role of sea ice in structuring Antarctic ecosystems, Polar Biol., 12, 3–13, https://doi.org/10.1007/BF00239960, 1992.

Eickhoff, L., Dreischmeier, K., Zipori, A., Sirotinskaya, V., Adar, C., Reicher, N., Braslavsky, I., Rudich, Y., and Koop, T.: Contrasting Behavior of Antifreeze Proteins: Ice Growth Inhibitors and Ice Nucleation Promoters, J. Phys. Chem. Lett., 10, 966–972, https://doi.org/10.1021/acs.jpclett.8b03719, 2019.

Ekman, A. M. and Schmale, J.: Aerosol processes in high-latitude environments and the effects on climate, in: Aerosols and climate, edited by: Carslaw, K. S., Elsevier, Amsterdam, Kidlington, Cambridge, MA, 651–706, 2022.

Garrison, D. and Buck, K.: The biota of Antarctic pack ice in the Weddell sea and Antarctic Peninsula regions, Polar Biol., 10, 211–219, https://doi.org/10.1007/BF00238497, 1989.

Gaudichet, A., Lefèvre, R., Gaudry, A., Ardouin, B., Lambert, G., and Miller, J.: Mineralogical composition of aerosols at Amsterdam Island, Tellus B, 41, 344–352, https://doi.org/10.1111/j.1600-0889.1989.tb00313.x, 1989.

Gersonde, R. and Zielinski, U.: The reconstruction of late Quaternary Antarctic sea-ice distribution – the use of diatoms as a proxy for sea-ice, Palaeogeogr. Palaeocl., 162, 263–286, https://doi.org/10.1016/S0031-0182(00)00131-0, 2000.

Govindarajan, A. G. and Lindow, S. E.: Size of Bacterial Ice-Nucleation Sites Measured in situ by Radiation Inactivation Analysis, P. Natl. Acad. Sci. USA, 85, 1334–1338, 1988.

Guillard, R. R. L. and Ryther, J. H.: Studies of marine planktonic diatoms: I. Cyclotella nana hustedt, and Detonula convervacea (cleve) gran, Can. J. Microbiol., 8, 229–239, https://doi.org/10.1139/m62-029, 1962.

Günther, S. and Dieckmann, G. S.: Vertical zonation and community transition of sea-ice diatoms in fast ice and platelet layer, Weddell Sea, Antarctica, Ann. Glaciol., 33, 287–296, https://doi.org/10.3189/172756401781818590, 2001.

Guo, S., Stevens, C. A., Vance, T. D. R., Olijve, L. L. C., Graham, L. A., Campbell, R. L., Yazdi, S. R., Escobedo, C., Bar-Dolev, M., Yashunsky, V., Braslavsky, I., Langelaan, D. N., Smith, S. P., Allingham, J. S., Voets, I. K., and Davies, P. L.: Structure of a 1.5-MDa adhesin that binds its Antarctic bacterium to diatoms and ice, Sci. Adv., 3, e1701440, https://doi.org/10.1126/sciadv.1701440, 2017.

Hartmann, M., Gong, X., Kecorius, S., van Pinxteren, M., Vogl, T., Welti, A., Wex, H., Zeppenfeld, S., Herrmann, H., Wiedensohler, A., and Stratmann, F.: Terrestrial or marine – indications towards the origin of ice-nucleating particles during melt season in the European Arctic up to 83.7° N, Atmos. Chem. Phys., 21, 11613–11636, https://doi.org/10.5194/acp-21-11613-2021, 2021.

Herbert, R. J., Murray, B. J., Whale, T. F., Dobbie, S. J., and Atkinson, J. D.: Representing time-dependent freezing behaviour in immersion mode ice nucleation, Atmos. Chem. Phys., 14, 8501–8520, https://doi.org/10.5194/acp-14-8501-2014, 2014.

Hiranuma, N., Augustin-Bauditz, S., Bingemer, H., Budke, C., Curtius, J., Danielczok, A., Diehl, K., Dreischmeier, K., Ebert, M., Frank, F., Hoffmann, N., Kandler, K., Kiselev, A., Koop, T., Leisner, T., Möhler, O., Nillius, B., Peckhaus, A., Rose, D., Weinbruch, S., Wex, H., Boose, Y., DeMott, P. J., Hader, J. D., Hill, T. C. J., Kanji, Z. A., Kulkarni, G., Levin, E. J. T., McCluskey, C. S., Murakami, M., Murray, B. J., Niedermeier, D., Petters, M. D., O'Sullivan, D., Saito, A., Schill, G. P., Tajiri, T., Tolbert, M. A., Welti, A., Whale, T. F., Wright, T. P., and Yamashita, K.: A comprehensive laboratory study on the immersion freezing behavior of illite NX particles: a comparison of 17 ice nucleation measurement techniques, Atmos. Chem. Phys., 15, 2489–2518, https://doi.org/10.5194/acp-15-2489-2015, 2015.

Hiranuma, N., Adachi, K., Bell, D. M., Belosi, F., Beydoun, H., Bhaduri, B., Bingemer, H., Budke, C., Clemen, H.-C., Conen, F., Cory, K. M., Curtius, J., DeMott, P. J., Eppers, O., Grawe, S., Hartmann, S., Hoffmann, N., Höhler, K., Jantsch, E., Kiselev, A., Koop, T., Kulkarni, G., Mayer, A., Murakami, M., Murray, B. J., Nicosia, A., Petters, M. D., Piazza, M., Polen, M., Reicher, N., Rudich, Y., Saito, A., Santachiara, G., Schiebel, T., Schill, G. P., Schneider, J., Segev, L., Stopelli, E., Sullivan, R. C., Suski, K., Szakáll, M., Tajiri, T., Taylor, H., Tobo, Y., Ullrich, R., Weber, D., Wex, H., Whale, T. F., Whiteside, C. L., Yamashita, K., Zelenyuk, A., and Möhler, O.: A comprehensive characterization of ice nucleation by three different types of cellulose particles immersed in water, Atmos. Chem. Phys., 19, 4823–4849, https://doi.org/10.5194/acp-19-4823-2019, 2019.

Hobbs, P. V.: 1. Introduction to atmospheric chemistry a companion text to Basic physical chemistry for the atmospheric sciences: A companion text to Basic physical chemistry for the atmospheric sciences, Cambridge University Press, Cambridge, 262 pp., 2000.

Hudait, A., Qiu, Y., Odendahl, N., and Molinero, V.: Hydrogen-Bonding and Hydrophobic Groups Contribute Equally to the Binding of Hyperactive Antifreeze and Ice-Nucleating Proteins to Ice, J. Am. Chem. Soc., 141, 7887–7898, https://doi.org/10.1021/jacs.9b02248, 2019.

Huebner, A., Srisa-Art, M., Holt, D., Abell, C., Hollfelder, F., deMello, A. J., and Edel, J. B.: Quantitative detection of protein expression in single cells using droplet microfluidics, Chem. Commun., 12, 1218–1220, https://doi.org/10.1039/b618570c, 2007.

Ickes, L., Porter, G. C. E., Wagner, R., Adams, M. P., Bierbauer, S., Bertram, A. K., Bilde, M., Christiansen, S., Ekman, A. M. L., Gorokhova, E., Höhler, K., Kiselev, A. A., Leck, C., Möhler, O., Murray, B. J., Schiebel, T., Ullrich, R., and Salter, M. E.: The ice-nucleating activity of Arctic sea surface microlayer samples and marine algal cultures, Atmos. Chem. Phys., 20, 11089–11117, https://doi.org/10.5194/acp-20-11089-2020, 2020.

Irish, V. E., Elizondo, P., Chen, J., Chou, C., Charette, J., Lizotte, M., Ladino, L. A., Wilson, T. W., Gosselin, M., Murray, B. J., Polishchuk, E., Abbatt, J. P. D., Miller, L. A., and Bertram, A. K.: Ice-nucleating particles in Canadian Arctic sea-surface microlayer and bulk seawater, Atmos. Chem. Phys., 17, 10583–10595, https://doi.org/10.5194/acp-17-10583-2017, 2017.

Irish, V. E., Hanna, S. J., Xi, Y., Boyer, M., Polishchuk, E., Ahmed, M., Chen, J., Abbatt, J. P. D., Gosselin, M., Chang, R., Miller, L. A., and Bertram, A. K.: Revisiting properties and concentrations of ice-nucleating particles in the sea surface microlayer and bulk seawater in the Canadian Arctic during summer, Atmos. Chem. Phys., 19, 7775–7787, https://doi.org/10.5194/acp-19-7775-2019, 2019.

Kang, S.-H. and Fryxell, G.: Fragilariopsis cylindrus (Grunow) Krieger: The most abundant diatom in water column assemblages of Antarctic marginal ice-edge zones, Polar Biol., 12, 609–627, https://doi.org/10.1007/BF00236984, 1992.

Knopf, D. A., Alpert, P. A., Wang, B., and Aller, J. Y.: Stimulation of ice nucleation by marine diatoms, Nat. Geosci, 4, 88–90, https://doi.org/10.1038/ngeo1037, 2011.

Kondo, H., Mochizuki, K., and Bayer-Giraldi, M.: Multiple binding modes of a moderate ice-binding protein from a polar microalga, Phys. Chem. Chem. Phys., 20, 25295–25303, https://doi.org/10.1039/c8cp04727h, 2018.

Koop, T.: Homogeneous Ice Nucleation in Water and Aqueous Solutions, Z. Phys. Chem., 218, 1231–1258, https://doi.org/10.1524/zpch.218.11.1231.50812, 2004.

Köster, S., Angilè, F. E., Duan, H., Agresti, J. J., Wintner, A., Schmitz, C., Rowat, A. C., Merten, C. A., Pisignano, D., Griffiths, A. D., and Weitz, D. A.: Drop-based microfluidic devices for encapsulation of single cells, Lab Chip, 8, 1110–1115, https://doi.org/10.1039/b802941e, 2008.

Krembs, C. and Engel, A.: Abundance and variability of microorganisms and transparent exopolymer particles across the ice-water interface of melting first-year sea ice in the Laptev Sea (Arctic), Marine Biology, 138, 173–185, https://doi.org/10.1007/s002270000396, 2001.

Krembs, C., Eicken, H., Junge, K., and Deming, J.: High concentrations of exopolymeric substances in Arctic winter sea ice: implications for the polar ocean carbon cycle and cryoprotection of diatoms, Deep Sea Res. Pt. I, 49, 2163–2181, https://doi.org/10.1016/S0967-0637(02)00122-X, 2002.

Krembs, C., Eicken, H., and Deming, J. W.: Exopolymer alteration of physical properties of sea ice and implications for ice habitability and biogeochemistry in a warmer Arctic, P. Natl. Acad. Sci. USA, 108, 3653–3658, https://doi.org/10.1073/pnas.1100701108, 2011.

Kunert, A. T., Pöhlker, M. L., Tang, K., Krevert, C. S., Wieder, C., Speth, K. R., Hanson, L. E., Morris, C. E., Schmale III, D. G., Pöschl, U., and Fröhlich-Nowoisky, J.: Macromolecular fungal ice nuclei in Fusarium: effects of physical and chemical processing, Biogeosciences, 16, 4647–4659, https://doi.org/10.5194/bg-16-4647-2019, 2019.

Leck, C. and Bigg, E. K.: Biogenic particles in the surface microlayer and overlaying atmosphere in the central Arctic Ocean during summer, Tellus B, 57, 305–316, https://doi.org/10.3402/tellusb.v57i4.16546, 2005.

Leck, C. and Bigg, E. K.: Comparison of sources and nature of the tropical aerosol with the summer high Arctic aerosol, Tellus B, 60, 118–126, https://doi.org/10.1111/j.1600-0889.2007.00315.x, 2008.

Lizotte, M. P.: The Contributions of Sea Ice Algae to Antarctic Marine Primary Production, Am Zool., 41, 57–73, https://doi.org/10.1093/icb/41.1.57, 2001.

Lundholm, N. and Hasle, G. R.: Are Fragilariopsis cylindrus and Fragilariopsis nana bipolar diatoms? – Morphological and molecular analyses of two sympatric species, Nova Hedwigia, Beiheft, 133, 231–250, 2008.

McCluskey, C. S., Hill, T. C. J., Humphries, R. S., Rauker, A. M., Moreau, S., Strutton, P. G., Chambers, S. D., Williams, A. G., McRobert, I., Ward, J., Keywood, M. D., Harnwell, J., Ponsonby, W., Loh, Z. M., Krummel, P. B., Protat, A., Kreidenweis, S. M., and DeMott, P. J.: Observations of Ice Nucleating Particles Over Southern Ocean Waters, Geophys. Res. Lett., 45, 11989–11997, https://doi.org/10.1029/2018GL079981, 2018.

Mock, T., Otillar, R. P., Strauss, J., McMullan, M., Paajanen, P., Schmutz, J., Salamov, A., Sanges, R., Toseland, A., Ward, B. J., Allen, A. E., Dupont, C. L., Frickenhaus, S., Maumus, F., Veluchamy, A., Wu, T., Barry, K. W., Falciatore, A., Ferrante, M. I., Fortunato, A. E., Glöckner, G., Gruber, A., Hipkin, R., Janech, M. G., Kroth, P. G., Leese, F., Lindquist, E. A., Lyon, B. R., Martin, J., Mayer, C., Parker, M., Quesneville, H., Raymond, J. A., Uhlig, C., Valas, R. E., Valentin, K. U., Worden, A. Z., Armbrust, E. V., Clark, M. D., Bowler, C., Green, B. R., Moulton, V., van Oosterhout, C., and Grigoriev, I. V.: Evolutionary genomics of the cold-adapted diatom Fragilariopsis cylindrus, Nature, 541, 536–540, https://doi.org/10.1038/nature20803, 2017.

Murray, B. J., O'Sullivan, D., Atkinson, J. D., and Webb, M. E.: Ice nucleation by particles immersed in supercooled cloud droplets, Chem. Soc. Rev., 41, 6519–6554, https://doi.org/10.1039/c2cs35200a, 2012.

Olenina, I., Hajdu, S., Edler, L., Andersson, A., Wasmund, N., Busch, S., Göbel, J., Gromisz, S., Huseby, S., Huttunen, M., Jaanus, A., Kokkonen, P., Ledaine, I., and Niemkiewicz, E.: Biovolumes and size-classes of phytoplankton in the Baltic Sea, HELCOM Balt. Sea Environ. Proc., 106, 144 pp., 2006.

O'Sullivan, D., Murray, B. J., Ross, J. F., Whale, T. F., Price, H. C., Atkinson, J. D., Umo, N. S., and Webb, M. E.: The relevance of nanoscale biological fragments for ice nucleation in clouds, Sci. Rep., 5, 8082, https://doi.org/10.1038/srep08082, 2015.

Pinti, V., Marcolli, C., Zobrist, B., Hoyle, C. R., and Peter, T.: Ice nucleation efficiency of clay minerals in the immersion mode, Atmos. Chem. Phys., 12, 5859–5878, https://doi.org/10.5194/acp-12-5859-2012, 2012.

Poulin, M., Daugbjerg, N., Gradinger, R., Ilyash, L., Ratkova, T., and Quillfeldt, C.: The pan-Arctic biodiversity of marine pelagic and sea-ice unicellular eukaryotes: a first-attempt assessment, Mar. Biodiv., 41, 13–28, https://doi.org/10.1007/s12526-010-0058-8, 2011.

Pummer, B. G., Bauer, H., Bernardi, J., Bleicher, S., and Grothe, H.: Suspendable macromolecules are responsible for ice nucleation activity of birch and conifer pollen, Atmos. Chem. Phys., 12, 2541–2550, https://doi.org/10.5194/acp-12-2541-2012, 2012.

Pummer, B. G., Budke, C., Augustin-Bauditz, S., Niedermeier, D., Felgitsch, L., Kampf, C. J., Huber, R. G., Liedl, K. R., Loerting, T., Moschen, T., Schauperl, M., Tollinger, M., Morris, C. E., Wex, H., Grothe, H., Pöschl, U., Koop, T., and Fröhlich-Nowoisky, J.: Ice nucleation by water-soluble macromolecules, Atmos. Chem. Phys., 15, 4077–4091, https://doi.org/10.5194/acp-15-4077-2015, 2015.

Rasmussen, D. H. and MacKenzie, A. P.: Effect of Solute on Ice-Solution Interfacial Free Energy; Calculation from Measured Homogeneous Nucleation Temperatures, in: Water Structure at the Water-Polymer Interface, Springer, Boston, MA, 126–145, 1972.

Raymond, J. A., Sullivan, C. W., and DeVries, A. L.: Release of an ice-active substance by Antarctic sea ice diatoms, Polar Biol., 14, 71–75, https://doi.org/10.1007/BF00240276, 1994.

Reicher, N., Segev, L., and Rudich, Y.: The WeIzmann Supercooled Droplets Observation on a Microarray (WISDOM) and application for ambient dust, Atmos. Meas. Tech., 11, 233–248, https://doi.org/10.5194/amt-11-233-2018, 2018.

Reicher, N., Budke, C., Eickhoff, L., Raveh-Rubin, S., Kaplan-Ashiri, I., Koop, T., and Rudich, Y.: Size-dependent ice nu-

cleation by airborne particles during dust events in the eastern Mediterranean, Atmos. Chem. Phys., 19, 11143–11158, https://doi.org/10.5194/acp-19-11143-2019, 2019.

Riechers, B., Wittbracht, F., Hütten, A., and Koop, T.: The homogeneous ice nucleation rate of water droplets produced in a microfluidic device and the role of temperature uncertainty, Phys. Chem. Chem. Phys., 15, 5873–5887, https://doi.org/10.1039/c3cp42437e, 2013.

Roy, P., Mael, L. E., Hill, T. C. J., Mehndiratta, L., Peiker, G., House, M. L., DeMott, P. J., Grassian, V. H., and Dutcher, C. S.: Ice Nucleating Activity and Residual Particle Morphology of Bulk Seawater and Sea Surface Microlayer, ACS Earth Space Chem., 5, 1916–1928, https://doi.org/10.1021/acsearthspacechem.1c00175, 2021.

Roy-Barman, M. and Jeandel, C.: Marine Geochemistry, Oxford University Press, ISBN 9780198787495, 2016.

Šantl-Temkiv, T., Lange, R., Beddows, D., Rauter, U., Pilgaard, S., Dall'Osto, M., Gunde-Cimerman, N., Massling, A., and Wex, H.: Biogenic Sources of Ice Nucleating Particles at the High Arctic Site Villum Research Station, Environ. Sci. Technol., 53, 10580–10590, https://doi.org/10.1021/acs.est.9b00991, 2019.

Šantl-Temkiv, T., Sikoparija, B., Maki, T., Carotenuto, F., Amato, P., Yao, M., Morris, C. E., Schnell, R., Jaenicke, R., Pöhlker, C., DeMott, P. J., Hill, T. C. J., and Huffman, J. A.: Bioaerosol field measurements: Challenges and perspectives in outdoor studies, Aerosol Sci. Tech., 54, 520–546, https://doi.org/10.1080/02786826.2019.1676395, 2020.

Seinfeld, J. H. and Pandis, S. N.: Atmospheric chemistry and physics: From air pollution to climate change, Third edition, Wiley, Hoboken, New Jersey, 1120 pp., 2016.

Steinke, I., DeMott, P. J., Deane, G. B., Hill, T. C. J., Maltrud, M., Raman, A., and Burrows, S. M.: A numerical framework for simulating the atmospheric variability of supermicron marine biogenic ice nucleating particles, Atmos. Chem. Phys., 22, 847–859, https://doi.org/10.5194/acp-22-847-2022, 2022.

Stohl, A. and Sodemann, H.: Characteristics of atmospheric transport into the Antarctic troposphere, J. Geophys. Res., 115, D02305, https://doi.org/10.1029/2009JD012536, 2010.

Tarn, M. D., Sikora, S. N. F., Porter, G. C. E., Shim, J.-U., and Murray, B. J.: Homogeneous Freezing of Water Using Microfluidics, Micromachines, 12, 223, https://doi.org/10.3390/mi12020223, 2021.

van Leeuwe, M. A., Tedesco, L., Arrigo, K. R., Assmy, P., Campbell, K., Meiners, K. M., Rintala, J.-M., Selz, V., Thomas, D. N., and Stefels, J.: Microalgal community structure and primary production in Arctic and Antarctic sea ice: A synthesis, Elementa, 6, 4, https://doi.org/10.1525/elementa.267, 2018.

Vance, T. D. R., Bayer-Giraldi, M., Davies, P. L., and Mangiagalli, M.: Ice-binding proteins and the "domain of unknown function" 3494 family, FEBS J., 286, 855–873, https://doi.org/10.1111/febs.14764, 2019.

Wagner, R., Ickes, L., Bertram, A. K., Els, N., Gorokhova, E., Möhler, O., Murray, B. J., Umo, N. S., and Salter, M. E.: Heterogeneous ice nucleation ability of aerosol particles generated from Arctic sea surface microlayer and surface seawater samples at cirrus temperatures, Atmos. Chem. Phys., 21, 13903–13930, https://doi.org/10.5194/acp-21-13903-2021, 2021.

Welti, A., Bigg, E. K., DeMott, P. J., Gong, X., Hartmann, M., Harvey, M., Henning, S., Herenz, P., Hill, T. C. J., Hornblow, B., Leck, C., Löffler, M., McCluskey, C. S., Rauker, A. M., Schmale, J., Tatzelt, C., van Pinxteren, M., and Stratmann, F.: Ship-based measurements of ice nuclei concentrations over the Arctic, Atlantic, Pacific and Southern oceans, Atmos. Chem. Phys., 20, 15191–15206, https://doi.org/10.5194/acp-20-15191-2020, 2020.

Wex, H., Augustin-Bauditz, S., Boose, Y., Budke, C., Curtius, J., Diehl, K., Dreyer, A., Frank, F., Hartmann, S., Hiranuma, N., Jantsch, E., Kanji, Z. A., Kiselev, A., Koop, T., Möhler, O., Niedermeier, D., Nillius, B., Rösch, M., Rose, D., Schmidt, C., Steinke, I., and Stratmann, F.: Intercomparing different devices for the investigation of ice nucleating particles using Snomax® as test substance, Atmos. Chem. Phys., 15, 1463–1485, https://doi.org/10.5194/acp-15-1463-2015, 2015.

Wilson, T. W., Ladino, L. A., Alpert, P. A., Breckels, M. N., Brooks, I. M., Browse, J., Burrows, S. M., Carslaw, K. S., Huffman, J. A., Judd, C., Kilthau, W. P., Mason, R. H., McFiggans, G., Miller, L. A., Nájera, J. J., Polishchuk, E., Rae, S., Schiller, C. L., Si, M., Temprado, J. V., Whale, T. F., Wong, J. P. S., Wurl, O., Yakobi-Hancock, J. D., Abbatt, J. P. D., Aller, J. Y., Bertram, A. K., Knopf, D. A., and Murray, B. J.: A marine biogenic source of atmospheric ice-nucleating particles, Nature, 525, 234–238, https://doi.org/10.1038/nature14986, 2015.

Wolber, P. K., Deininger, C. A., Southworth, M. W., Vandekerckhove, J., van Montagu, M., and Warren, G. J.: Identification and Purification of a Bacterial Ice-Nucleation Protein, P. Natl. Acad. Sci. USA, 83, 7256–7260, 1986.

Xi, Y., Mercier, A., Kuang, C., Yun, J., Christy, A., Melo, L., Maldonado, M. T., Raymond, J. A., and Bertram, A. K.: Concentrations and properties of ice nucleating substances in exudates from Antarctic sea-ice diatoms, Environ. Sci., 23, 323–334, https://doi.org/10.1039/d0em00398k, 2021.